

# NASA Contractor Report 157136

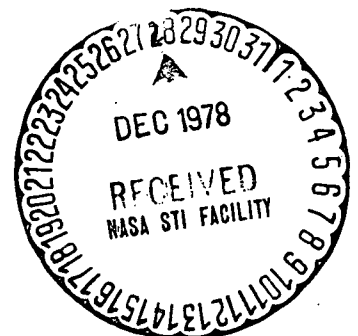
STRESS INTENSITY FACTORS IN A CRACKED INFINITE  
ELASTIC WEDGE LOADED BY A RIGID PUNCH

F. Erdogan and M. B. Civelek

LEHIGH UNIVERSITY  
Bethlehem, PA 18015

NASA Grant NGR 39-007-011  
May 1978

**NASA**  
National Aeronautics and  
Space Administration  
**Langley Research Center**  
Hampton, Virginia 23665



STRESS INTENSITY FACTORS IN A  
CRACKED INFINITE ELASTIC WEDGE  
LOADED BY A RIGID PUNCH\*

by

F. Erdogan and M. Basar Civelek  
Lehigh University, Bethlehem, Pa. 18015

ABSTRACT

The paper considers splitting a plane elastic wedge-shaped solid through the application of a rigid punch. It is assumed that the coefficient of friction on the contact area is constant, the problem has a plane of symmetry with respect to loading and geometry, and the crack lies in the plane of symmetry. The problem is formulated in terms of a system of integral equations with the contact stress and the derivative of the crack surface displacement as the unknown functions. The solution is obtained for an internal crack and for an edge crack. The results include primarily the stress intensity factors at the crack tips, and the measure of the stress singularity at the wedge apex, and at the end points of the contact area.

---

\* This work was supported by the National Aeronautics and Space Administration under the Grant NGR39-007-011 and by the National Science Foundation under the Grant ENG77-19127.

## 1. INTRODUCTION

In structural and mechanical design the importance of stress concentration around notches has long been well recognized and the related theoretical problems have been extensively studied (e.g. [1]). Conforming to a sound design practice, in most of these studies it is assumed that the radius of curvature of the notch is greater than zero. However, in failure studies where normally brittle fracture would be the expected mode of failure, it may be convenient and perhaps even necessary to study the limiting case of the problem in which the radius of curvature of the notch is zero. This problem too has been studied rather extensively by assuming that the relevant portion of the solid may be approximated by an infinite elastic wedge with a given notch angle (e.g. [2,3], for additional references see [4]). Most of these studies deal with the solution of the related traction and/or displacement boundary value problems. However, in real problems the external load is applied to the component usually through another solid contacting the wedge. In these problems if the contact region is sufficiently close to the apex of the wedge, it is clear that the stress concentration factor or the parameter representing the strength of the stress singularity would depend on the details of the distribution of contact stresses as well as on the resultant forces. Such contact problems

for elastic wedges without or with taking into account the effect of friction were considered in [4] and [5]. A slightly different problem dealing with the process of wedge-splitting of a semi-infinite strip was considered in [6].

The results given in [4] and [5] may be used in brittle wedge-shaped solids to study the initiation of fracture at the wedge apex. To deal with the problem after fracture initiation one needs the solution of the corresponding crack-contact problem. For the symmetric geometry shown in Figure 1 and under symmetric loading conditions the problem is considered in this paper. In formulating the problem it is assumed that the driving punch through which the load is applied is rigid and the coefficient of friction along the contact area is constant. More recently, the traction boundary value problem for an infinite wedge containing an edge crack was considered in [7], where the problem is solved for uniform pressure on the wedge and the crack surfaces. The nature of the external loads considered in [7] however, appears to limit the practical usefulness of its results.

## 2. FORMULATION

Consider the plane elastostatic problem for the infinite wedge-shaped domain of angle  $2\theta_0$  shown in Figure 1.

The external load  $P_0$  is applied to the medium through a rigid punch with known profile. It is assumed that  $(\theta=0, \theta=\pi)$  is a plane of symmetry with respect to geometry as well as loading. If the magnitude of the load  $P_0$  is increased beyond a certain value, then a crack may develop along  $\theta=0$  plane. This may be the consequence of cyclic loading or, in "brittle" materials such as rocks, ceramics, and a rather large variety of cast metal alloys, it may result from the static application of the load. Generally, the crack would start from the apex of the wedge as an "edge crack." However, the problem will be formulated for the internal crack geometry shown in Figure 1 and the edge crack will be treated as the limiting case for  $c \rightarrow 0$ . In this problem, because of symmetry it is sufficient to consider one-half of the medium only. First the problem will be formulated for the general case in which the normal and tangential components of the unknown contact stress vector are independent of each other. This formulation is necessary to solve the problem in which due to a very high coefficient of friction, no sliding may take place between the punch and the elastic wedge. In this case the plane elasticity problem must be solved under the following boundary conditions:

$$\sigma_{\theta\theta}(r, \theta_0) = 0 \quad , \quad 0 < r < a \quad , \quad b < r < \infty \quad , \quad (1a)$$

$$\frac{\partial}{\partial r} u_{\theta}(r, \theta_0) = \frac{1+\kappa}{4\mu} g_1(r) \quad , \quad a < r < b \quad , \quad (1b)$$

$$\sigma_{r\theta}(r, \theta_0) = 0 \quad , \quad 0 < r < a \quad , \quad b < r < \infty \quad (2a)$$

$$\frac{\partial}{\partial r} u_r(r, \theta_0) = \frac{1+\kappa}{4\mu} g_2(r) \quad , \quad a < r < b \quad , \quad (2b)$$

$$\sigma_{r\theta}(r, 0) = 0 \quad , \quad 0 < r < \infty \quad , \quad (3)$$

$$u_\theta(r, 0) = 0 \quad , \quad 0 < r < c \quad , \quad d < r < \infty \quad , \quad (4a)$$

$$\sigma_{\theta\theta}(r, 0) = g_3(r) \quad , \quad c < r < d \quad , \quad (4b)$$

where  $\mu$  is the shear modulus,  $\kappa=3-4\nu$  for plane strain and  $\kappa=(3-\nu)/(1+\nu)$  for generalized plane stress, and  $g_1$ ,  $g_2$ , and  $g_3$  are known functions.

The problem is formulated by using the Mellin transforms. Defining the stress and displacement combinations

$$\sigma(r, \theta) = \sigma_{r\theta} + i\sigma_{\theta\theta} \quad , \quad v(r, \theta) = \frac{\partial}{\partial r} (u_r + iu_\theta) \quad , \quad (5a, b)$$

for an elastic wedge one may easily obtain (see, for example, [8])

$$M[r^2\sigma] = 2i(s+1)[Ase^{is\theta} + B(s+1)e^{i(s+2)\theta} - \bar{B}e^{-i(s+2)\theta}] \quad , \quad (6)$$

$$M[r^2v] = -\frac{s+1}{\mu} [Ase^{is\theta} + B(s+1)e^{i(s+2)\theta} + \kappa\bar{B}e^{-i(s+2)\theta}] \quad . \quad (7)$$

where for a given function  $f(r)$  the Mellin transforms are defined by

$$M[f] = \int_0^{\infty} f(r)r^{s-1}dr \quad , \quad f(r) = \frac{1}{2\pi i} \int_{c_0-i\infty}^{c_0+i\infty} M[f]r^{-s}ds \quad , \quad (8)$$

provided the strip of regularity containing the constant  $c_0$  is selected in such a way that, considered together with the behavior of  $f(r)$  as  $r \rightarrow 0$  and  $r \rightarrow \infty$ , the integrals exist. In (6) and (7) the complex functions  $A(s)$  and  $B(s)$  are unknown and are determined from the four boundary conditions specified along  $\theta=0$  and  $\theta=\theta_0$ . In the problem under consideration there are one homogeneous (i.e., condition (3)) and three mixed boundary conditions (i.e., (1), (2) and (4)). Thus, substituting from (6) and (7) into (1)-(4), one could eliminate one of the four real unknown functions and obtain a system of three simultaneous dual integral equations for the remaining three unknowns. Since the problem involves singularities with powers other than  $\mp 1/2$ , this would not be the proper way to try to solve the problem. On the other hand, defining

$$f_1(r) = \sigma_{\theta\theta}(r, \theta_0) \quad , \quad 0 < r < \infty \quad , \quad (9)$$

$$f_2(r) = \sigma_{r\theta}(r, \theta_0) \quad , \quad 0 < r < \infty \quad , \quad (10)$$

$$f_3(r) = \frac{4\mu}{1+\kappa} \frac{\partial}{\partial r} u_{\theta}(r, 0) \quad , \quad 0 < r < \infty \quad , \quad (11)$$

and replacing the conditions (1), (2), and (4), respectively by (9), (10), and (11), one may easily determine the complex

functions  $A(s)$  and  $B(s)$  and, as a result, all the relevant field quantities such as  $\sigma(r,\theta)$  and  $v(r,\theta)$  in terms of  $f_1$ ,  $f_2$ , and  $f_3$ . From (1a), (2a), and (4a) we observe that  $f_1$ ,  $f_2$ , and  $f_3$  are zero on the infinite portion of the interval  $0 < r < \infty$ , and are unknown on the remaining part. Using now the boundary conditions (1b), (2b), and (4b) which have not yet been satisfied, we could obtain a system of integral equations having finite supports to determine these functions. The analysis leading to the integral equations is somewhat lengthy and will not be given in this paper. The derivations and the asymptotic analysis follow very closely and partially repeat the procedure outlined in [4], [5], and [6]. Thus, for the problem described in Figure 1 the boundary conditions (1b), (2b), and (4b) give the following integral equations to determine the unknown functions  $f_1$ ,  $f_2$ , and  $f_3$ :

$$g_1(r) = -\left(\frac{\kappa-1}{\kappa+1}\right) f_2(r) + \frac{1}{\pi} \int_a^b \left\{ \left[ \frac{1}{r\rho} + k_{11}(r,t) \right] f_1(t) + k_{12}(r,t) f_2(t) \right\} dt + \frac{1}{\pi} \int_c^d k_{13}(r,t) f_3(t) dt \quad , \quad a < r < b \quad , \quad (12)$$

$$g_2(r) = \left(\frac{\kappa-1}{\kappa+1}\right) f_1(r) + \frac{1}{\pi} \int_a^b \left\{ k_{21}(r,t) f_1(t) + \left[ \frac{1}{r\rho} + k_{22}(r,t) \right] f_2(t) \right\} dt + \frac{1}{\pi} \int_c^d k_{23}(r,t) f_3(t) dt \quad , \quad a < r < b \quad , \quad (13)$$



$$g_3(r) = \frac{1}{\pi} \int_a^b [k_{31}(r,t)f_1(t) + k_{32}(r,t)f_2(t)]dt \\ + \frac{1}{\pi} \int_c^d \left[ \frac{1}{r\rho} + k_{33}(r,t) \right] f_3(t)dt \quad , \quad c < r < d \quad , \quad (14)$$

where

$$\rho = \log(t/r) \quad , \quad (15)$$

and the Fredholm kernels  $k_{ij}(i,j=1,2,3)$  are given by

$$k_{11}(r,t) = - \frac{\pi \sin^2 \theta_0}{r(2\theta_0 + \sin 2\theta_0)} + \int_0^\infty \left( \frac{\cosh 2\theta_0 y - \cos 2\theta_0}{D(y)} - 1 \right) \\ \times \frac{\sin \rho y}{r} dy \quad ,$$

$$k_{12}(r,t) = \frac{\pi \sin \theta_0 \cos \theta_0}{r(2\theta_0 + \sin 2\theta_0)} - \int_0^\infty \frac{\sin 2\theta_0}{rD(y)} \sin \rho y dy \\ - \int_0^\infty \left( \frac{\sinh 2\theta_0 y}{D(y)} - 1 \right) \frac{\cos \rho y}{r} dy \quad ,$$

$$k_{13}(r,t) = 2 \int_0^\infty \frac{\cos \theta_0 \sinh \theta_0 y + y \sin \theta_0 \cosh \theta_0 y}{rD(y)} \cos \rho y dy \quad ,$$

$$k_{21}(r,t) = k_{12}(r,t) \quad ,$$

$$k_{22}(r,t) = - \frac{\pi \cos^2 \theta_0}{r(2\theta_0 + \sin 2\theta_0)} + \int_0^\infty \left( \frac{\cosh 2\theta_0 y + \cos 2\theta_0}{D(y)} - 1 \right) \\ \times \frac{\sin \rho y}{r} dy \quad ,$$

$$k_{23}(r,t) = 2 \int_0^\infty \frac{\sin \theta_0 \sinh \theta_0 y}{rD(y)} (\cos \rho y - y \sin \rho y) dy \quad ,$$

$$k_{31}(r,t) = k_{13}(r,t) \quad ,$$

$$k_{32}(r,t) = 2 \int_0^{\infty} \frac{\sin\theta_0 \sinh\theta_0 y}{rD(y)} (\cos\theta_0 y + y \sin\theta_0 y) dy ,$$

$$k_{33}(r,t) = \int_0^{\infty} \left( \frac{\cosh 2\theta_0 y - 1 - y^2 (1 - \cos 2\theta_0)}{D(y)} - 1 \right) \frac{\sin\theta_0 y}{r} dy ,$$

(16a-i)

$$D(y) = \sinh 2\theta_0 y + y \sin 2\theta_0 .$$

(17)

From the definition of  $f_3$  as given by (11) and the boundary condition (4a) it is clear that for  $c > 0$   $f_3$  must satisfy the following single-valuedness condition:

$$\int_c^d f_3(t) dt = 0 .$$

(18)

Also, the force equilibrium along the contact area requires that

$$\int_a^b f_1(t) dt = -P ,$$

(19)

$$\int_a^b f_2(t) dt = -Q ,$$

(20)

where  $P$  and  $Q$  are the normal and the tangential components of the resultant contact force. Thus, the integral equations (12-14) must be solved under conditions (18-20).

In the case of constant coefficient friction  $\eta$

$$Q = \eta P ,$$

(21)

$$P = P_0 / [2 \sin(\pi - \theta_0) + 2 \eta \cos(\pi - \theta_0)] ,$$

(22)

where  $P_0$  is the driving force shown in Figure 1. In the no-slip case (i.e., for perfect adhesion)  $f_1$  and  $f_2$ , and consequently,  $P$  and  $Q$  are independent and are determined from the following equilibrium and kinematic compatibility conditions:\*

$$P \sin(\pi - \theta_0) + Q \cos(\pi - \theta_0) = P_0/2 \quad , \quad (23)$$

$$\tan(\pi - \theta_0) = u_\theta(a, \theta_0)/u_r(a, \theta_0) \quad . \quad (24)$$

Examining the behavior of the term  $1/r\rho$  in the kernels it may be shown that

$$\begin{aligned} \frac{1}{r\rho} &= \frac{1}{r \log(t/r)} = \frac{1}{r(\frac{t}{r} - 1)} \left[ 1 + \sum_1^{\infty} \frac{(-1)^n}{n+1} \left(\frac{t}{r} - 1\right)^n \right]^{-1} \\ &= \frac{1}{t-r} [1 + O(\frac{t}{r} - 1)] \quad . \end{aligned} \quad (25)$$

Thus, the integral equations (12-14) are singular with Cauchy type kernels. Also, one may note that the dominant part of (12) and (13) is identical to the coupled integral equations for an elastic half plane loaded by a perfectly adhering rigid punch, and that of (14) is the integral equation for the crack in an infinite plane.

If the contact under the punch is frictionless, then

---

\* Note that in this case the contact surface moves by a rigid body displacement parallel to the  $\theta=0$  plane. Therefore, the kinematic relation can be written at any point on the contact surface.

$f_2(r)=0$  and (12) and (14) give the system of singular integral equations to determine the unknown functions  $f_1$  and  $f_3$ . In this case the additional conditions are (18) and the following equilibrium relation:

$$\int_a^b f_1(t)dt = -P_0/2\sin(\pi-\theta_0) \quad (26)$$

On the other hand, if the punch is driven with constant coefficient of friction  $\eta$ , we have

$$f_2(t) = \eta f_1(t) \quad (27)$$

$$g_1(r) = -\gamma f_1(r) + \frac{1}{\pi} \int_a^b \left[ \frac{1}{r\rho} + k_{11}(r,t) + \eta k_{12}(r,t) \right] f_1(t) dt + \frac{1}{\pi} \int_c^d k_{13}(r,t) f_3(t) dt \quad , \quad a < r < b \quad , \quad (28)$$

$$g_3(r) = \frac{1}{\pi} \int_a^b [k_{31}(r,t) + \eta k_{32}(r,t)] f_1(t) dt + \frac{1}{\pi} \int_c^d \left[ \frac{1}{r\rho} + k_{33}(r,t) \right] f_3(t) dt \quad , \quad c < r < d \quad , \quad (29)$$

$$\gamma = \eta(\kappa-1)/(\kappa+1) \quad , \quad (30)$$

where the kernels  $k_{ij}$  are given by (16). In this problem (28) and (29) must be solved under conditions (18) and (22).

### 3. STRESS SINGULARITIES

Referring to Figure 1 the stress state is expected to be singular at the crack tips  $c$  and  $d$  and at the wedge apex  $O$ .

Defining the stress intensity factors at the crack tips by

$$k(c) = \lim_{r \rightarrow c} \sqrt{2(c-r)} \sigma_{\theta\theta}(r,0) ,$$

$$k(d) = \lim_{r \rightarrow d} \sqrt{2(r-d)} \sigma_{\theta\theta}(r,0) , \quad (31a,b)$$

and noting that in (14)  $g_3(r) = \sigma_{\theta\theta}(r,0)$  outside as well as inside the interval  $c < r < d$ , one may easily show that only the dominant term in the integral equation would contribute to the singularity giving [9]

$$k(c) = \lim_{r \rightarrow c} \sqrt{2(r-c)} f_3(r) , \quad (32)$$

$$k(d) = -\lim_{r \rightarrow d} \sqrt{2(d-r)} f_3(r) . \quad (33)$$

If  $c > 0$ , the wedge apex is also a point of stress singularity. Perhaps the easiest way to extract this singularity would be going back to (6) and expressing  $\sigma_{\theta\theta}$  in terms of  $f_1$ ,  $f_2$ , and  $f_3$ . Thus, after some simple manipulations we find

$$r\sigma_{\theta\theta}(r,0) = \int_a^b [K_1(r,t)f_1(t) + K_2(r,t)f_2(t)]dt$$

$$+ \int_c^d K_3(r,t)f_3(t)dt , \quad (34)$$

$$K_j(r,t) = \frac{1}{2\pi i} \int_{c_0 - i\infty}^{c_0 + i\infty} \left(\frac{t}{r}\right)^{s+1} \frac{F_j(s)}{\Delta(s)} ds , \quad (35)$$

$$\Delta(s) = (s+1)\sin 2\theta_0 + \sin 2(s+1)\theta_0 ,$$

$$F_1(s) = (s+2)\sin(s+2)\theta_0 - s\sin s\theta_0 ,$$

$$F_2(s) = s \cos(s+2)\theta_0 - s \cos s \theta_0 ,$$

$$F_3(s) = s(s+2) - (s+1)^2 \cos 2\theta_0 + \cos 2(s+1)\theta_0 , \quad (36a-d)$$

where the strip of regularity for Mellin inversion integrals is given by [4,5]

$$\operatorname{Re}(s_{-1}) < \operatorname{Re}(s) = c_0 < -1 \quad (37)$$

$s_{-1}$  being the first root of  $\Delta(s)=0$  to the left of the line  $\operatorname{Re}(s)=-1$ . For small values of  $r$ ,  $t > r$  and consequently to evaluate the integrals in (35) the contour must be closed to the left. Therefore, from (34) and (35) it is seen that the leading term in the infinite series giving the stress will be

$$\sigma_{\theta\theta}(r,0) \sim r^{-\omega} , \quad \omega = 2 + s_{-1} , \quad -2 < s_{-1} < -1 . \quad (38)$$

Thus, defining the strength of the stress singularity by

$$k(0) = \lim_{r \rightarrow 0} r^\omega \sigma_{\theta\theta}(r,0) \quad (39)$$

we obtain

$$k(0) = \frac{F_1(s_{-1})}{\Delta'(s_{-1})} \int_a^b f_1(t) t^{1+s_{-1}} dt + \frac{F_2(s_{-1})}{\Delta'(s_{-1})} \int_a^b f_2(t) t^{1+s_{-1}} dt + \frac{F_3(s_{-1})}{\Delta'(s_{-1})} \int_c^d f_3(t) t^{1+s_{-1}} dt , \quad (40)$$

where

$$\Delta'(s) = \sin 2\theta_0 + 2\theta_0 \cos 2(s+1)\theta_0 \quad (41)$$

4. SPECIAL CASES:  $\theta_0 = \pi$ ,  $\theta_0 = \pi/2$

In the special cases of the plane with a semi-infinite crack ( $\theta_0 = \pi$ ) and the half plane ( $\theta_0 = \pi/2$ ), the kernels can be evaluated in closed form, simplifying the integral equations quite considerably. This requires the evaluation of a number of relatively simple Fourier integrals (see for example, [5]). Thus, for example, for  $\theta_0 = \pi$  the integral equations (28) and (29) become

$$g_1(r) = -\gamma f_1(r) + \frac{1}{\pi} \int_a^b \frac{1}{t-r} (t/r)^{1/2} f_1(t) dt - \frac{2}{\pi} \int_c^d \frac{1}{t+r} (t/r)^{1/2} f_3(t) dt, \quad a < r < b, \quad (42)$$

$$g_3(r) = -\frac{2}{\pi} \int_a^b \frac{1}{t+r} (t/r)^{1/2} f_1(t) dt + \frac{1}{\pi} \int_c^d \frac{1}{t-r} (t/r)^{1/2} f_3(t) dt, \quad c < r < d. \quad (43)$$

Similarly for  $\theta_0 = \pi/2$  we find

$$g_1(r) = -\gamma f_1(r) + \frac{1}{\pi} \int_a^b \frac{2r}{t^2 - r^2} f_1(t) dt + \frac{1}{\pi} \int_c^d \frac{4rt^2}{(t^2 + r^2)^2} f_3(t) dt, \quad a < r < b, \quad (44)$$

$$g_3(r) = \frac{1}{\pi} \int_a^b \frac{4t^2(r+nt)}{(t^2 + r^2)^2} f_1(t) dt + \frac{1}{\pi} \int_c^d \left[ \frac{1}{t-r} + \frac{4tr+r^2-t^2}{(t+r)^3} \right] f_3(t) dt, \quad c < r < d. \quad (45)$$

Equations (42-45) reduce to the integral equations for the well-known crack and contact problems if the crack and contact regions are taken sufficiently far apart. For example, in (42) and (43) if  $c \rightarrow \infty$ ,  $d \rightarrow \infty$  with  $d-c = \text{finite}$ , the coupling terms vanish and the uncoupled equations become that of a punch in a semi-infinite crack given in [5] and that of a crack in an infinite solid (which has only a simple Cauchy kernel). Similarly, in (44) and (45) for  $c \rightarrow \infty$ ,  $d \rightarrow \infty$ ,  $d-c = \text{finite}$  the coupling terms and the second term in (45) vanish giving again the known equations of two symmetric punches on a half plane and a crack in an infinite plane. Also, for  $a \rightarrow \infty$ ,  $b \rightarrow \infty$ ,  $b-a = \text{finite}$ , the coupling terms again vanish, (44) reduces to the integral equation for a single punch on a half-plane (which would now have in addition to the term  $\gamma f_1$  only a Cauchy kernel), and (45) becomes the integral equation of a semi-infinite plane having a crack perpendicular to the boundary (see, for example [10]).

In a half plane subjected to compression through rigid punches, since normally  $\theta=0$  plane would be under compression, the case of  $\theta_0 = \pi/2$  may not be very practical.



## 5. THE NUMERICAL SOLUTION

The dominant part of the singular integral equations (14) and (29) is of the first kind, is not coupled with that of the remaining equations in the system, and has only a simple Cauchy-type kernel. Since the singular behavior of the solution is dependent on the dominant part of the integral equations only, the unknown function  $f_3(r)$  would have as expected, standard square root singularity. The dominant parts of (12) and (13) are coupled and the integral equations are of the second kind. By defining

$$f(r) = f_1(r) + if_2(r) \quad , \quad a < r < b \quad (46)$$

the dominant parts can be combined and the solution may be expressed as

$$f(r) = F(r) (b-r)^\alpha (r-a)^\beta \quad , \quad -1 < \text{Re}(\alpha, \beta) < 1 \quad (47)$$

where  $F(r)$  is bounded in  $a \leq r \leq b$ .

Similarly, from (29) it follows that [9]

$$f_1(r) = F_1(r) (b-r)^\alpha (r-a)^\beta \quad , \quad -1 < \text{Re}(\alpha, \beta) < 1 \quad (48)$$

where, again  $F_1(r)$  is bounded in  $a \leq r \leq b$ . The constants  $\alpha$  and  $\beta$  may be determined following the standard function-theoretic method (see, for example, [9]). The numerical values of  $\alpha$  and  $\beta$  and the index of the integral equations (12), (13), and (28) would depend on the conditions of contact and the profile of the punch. These values are tabulated in Table 1 where  $\eta = \infty$  corresponds to the perfect


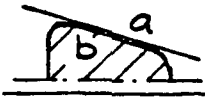
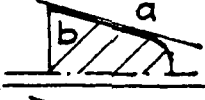
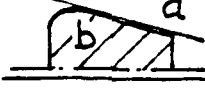
adhesion case (in which  $f_1$  and  $f_2$  are independent) and the constants  $\Omega$  and  $\omega_0$  are defined by

$$\tan \Omega = \frac{\kappa+1}{\eta(\kappa-1)}, \quad \omega_0 = \frac{\log \kappa}{2\pi}$$

One may note that in the case of constant coefficient of friction  $\alpha$  and  $\beta$  are always real, whereas in the perfect adhesion case they are complex and hence the singularity is of oscillating type.

The numerical results given in this paper are for the case of constant coefficient of friction. The corresponding

Table 1. Values of  $\alpha$  and  $\beta$

	Index	$\eta = 0$		$\eta = \text{constant}$		$\eta = \infty$	
		$\alpha$	$\beta$	$\alpha$	$\beta$	$\alpha$	$\beta$
	1	$-\frac{1}{2}$	$-\frac{1}{2}$	$\frac{\Omega}{\pi}-1$	$-\frac{\Omega}{\pi}$	$-\frac{1}{2}-i\omega_0$	$-\frac{1}{2}+i\omega_0$
	-1	$\frac{1}{2}$	$\frac{1}{2}$	$\frac{\Omega}{\pi}$	$1-\frac{\Omega}{\pi}$	$\frac{1}{2}-i\omega_0$	$\frac{1}{2}+i\omega_0$
	0	$-\frac{1}{2}$	$\frac{1}{2}$	$\frac{\Omega}{\pi}-1$	$1-\frac{\Omega}{\pi}$	$-\frac{1}{2}-i\omega_0$	$\frac{1}{2}+i\omega_0$
	0	$\frac{1}{2}$	$-\frac{1}{2}$	$\frac{\Omega}{\pi}$	$-\frac{\Omega}{\pi}$	$\frac{1}{2}-i\omega_0$	$-\frac{1}{2}+i\omega_0$

integral equations are (28) and (29) which must be solved under conditions (18) and (19). The solution is obtained by using the Gauss-Chebyshev and Gauss-Jacobi integration formulas described, for example, in [9]. Before using

these formulas the intervals in (28) and (29) are normalized by defining

$$\begin{aligned}
 x_1 &= \frac{2r}{b-a} - \frac{b+a}{b-a} , \quad s_1 = \frac{2t}{b-a} - \frac{b+a}{b-a} , \quad a < (r,t) < b , \\
 x_2 &= \frac{2r}{d-c} - \frac{d+c}{d-c} , \quad s_2 = \frac{2t}{d-c} - \frac{d+c}{d-c} , \quad c < (r,t) < d , \\
 \phi_1(s_1) &= f_1(t)/p_0 , \quad \phi_2(s_2) = f_3(t)/p_0 , \\
 \psi_1(x_1) &= g_1(r)/p_0 , \quad \psi_2(x_2) = g_3(r)/p_0 , \\
 p_0 &= 2P/(b-a) , \quad -1 < (x_1, x_2, s_1, s_2) < 1 . \quad (50)
 \end{aligned}$$

Thus, equations (28), (29), (19) and (18) may be replaced by

$$\begin{aligned}
 \psi_1(x_1) &= -\gamma\phi_1(x_1) + \frac{1}{\pi} \int_{-1}^1 h_{11}(x_1, s_1) \phi_1(s_1) ds_1 \\
 &\quad + \frac{1}{\pi} \int_{-1}^1 h_{12}(x_1, s_2) \phi_2(s_2) ds_2 , \quad -1 < x_1 < 1 ,
 \end{aligned}$$

$$\begin{aligned}
 \psi_2(x_2) &= \frac{1}{\pi} \int_{-1}^1 h_{21}(x_2, s_1) \phi_1(s_1) ds_1 \\
 &\quad + \frac{1}{\pi} \int_{-1}^1 h_{22}(x_2, s_2) \phi_2(s_2) ds_2 , \quad -1 < x_2 < 1 , \quad (51 \text{ a,b})
 \end{aligned}$$

$$\int_{-1}^1 \phi_1(s_1) ds_1 = -1 ,$$

$$\int_{-1}^1 \phi_2(s_2) ds_2 = 0 , \quad (52 \text{ a,b})$$

Where the kernels  $h_{ij}$ , ( $i, j=1,2$ ) are obtained by comparing the respective terms in (28) and (51a), and (29) and (51b).

Defining now

$$\begin{aligned}
 \phi_1(s_1) &= G_1(s_1)(1-s_1)^\alpha(1+s_1)^\beta , \\
 \phi_2(s_2) &= G_2(s_2)(1-s_2^2)^{-\frac{1}{2}} , \quad (53 \text{ a,b})
 \end{aligned}$$

and using the quadrature formulas given in [9], (51) and (52) become

$$\sum_{k=1}^n [H_k h_{11}(x_{1i}, s_{1k}) G_1(s_{1k}) + W_k h_{12}(x_{1i}, s_{2k}) G_2(s_{2k})] = \pi \psi_1(x_{1i}) ,$$

$$\sum_{k=1}^n [H_k h_{21}(x_{2i}, s_{1k}) G_1(s_{1k}) + W_k h_{22}(x_{2i}, s_{2k}) G_2(s_{2k})] = \pi \psi_2(x_{2i}) , \quad i = 1, \dots, n-1 , \quad (54 \text{ a,b})$$

$$\sum_{k=1}^n H_k G_1(s_{1k}) = -1 , \quad \sum_{k=1}^n W_k G_2(s_{2k}) = 0 , \quad (55 \text{ a,b})$$

where it is assumed that the punch has "sharp" corners.

Hence,  $\alpha = (\Omega/\pi) - 1$  and  $\beta = -\Omega/\pi$  (see Table 1). The weights, integration points, and collocation points which appear in (54) and (55) are given by [9]

$$H_1 = \frac{(1+\alpha)[\Gamma(1+\alpha)]^2 \Gamma(n+\beta)}{(n-1)\Gamma(n+\alpha)} ;$$

$$H_2 = \frac{(1+\beta)[\Gamma(1+\beta)]^2 \Gamma(n+\alpha)}{(n-1)\Gamma(n+\beta)} ;$$

$$H_k = \frac{2^{2+\alpha+\beta}}{1-s_{1k}^2} \frac{\Gamma(n-1+\alpha)\Gamma(n-1+\beta)}{(n-2)!\Gamma(n+1+\alpha+\beta)} \times$$

$$\times \frac{2n-2+\alpha+\beta}{P_{n-3}^{(1+\alpha, 1+\beta)}(s_{1k}) \frac{d}{ds_1} P_{n-2}^{(1+\alpha, 1+\beta)}(s_{1k})} ,$$

$$k = 2, \dots, n-1 ;$$

$$s_{11} = 1 , \quad s_{1n} = -1 , \quad P_{n-2}^{(1+\alpha, 1+\beta)}(s_{1k}) = 0 ,$$

$$k = 2, \dots, n-1 ;$$

$$p_{n-1}^{(-1-\alpha, -1-\beta)}(x_{1i}) = 0, \quad i = 1, \dots, n-1;$$

$$W_1 = W_n = \frac{\pi}{2(n-1)}; \quad W_k = \frac{\pi}{n-1}, \quad k = 2, \dots, n-1;$$

$$s_{2k} = \cos\left(\pi \frac{k-1}{n-1}\right), \quad k = 1, \dots, n;$$

$$x_{2i} = \cos\left(\pi \frac{2i-1}{2n-2}\right), \quad i = 1, \dots, n-1. \quad (56)$$

Equations (54) and (55) give  $2n$  linear algebraic equations to determine the unknowns  $G_1(s_{1k})$  and  $G_2(s_{2k})$ ,  $k = 1, \dots, n$ .

In all the examples given in this paper it is assumed that the crack surfaces are traction-free. Therefore,  $g_3 = 0$  or  $\psi_2(x_2) = 0$ . Also, in a flat-ended punch with sharp corners  $\psi_1(x_1)$  too is zero.

For a blunted punch which consists of a flat face and a rounded nose with radius  $R$  in the contact region the input function  $g_1(r)$  is given by (see the insert in Figure 7)

$$g(r) = \begin{cases} \frac{4\mu}{1+\kappa} \frac{r-a_0}{R}, & a < r < a_0 \\ 0, & a_0 < r < b \end{cases} \quad (57)$$

where  $a_0$ ,  $b$ , and  $R$  are known constants and  $a$  is unknown. In this case the index of the integral equation (28) is zero (see Table 1), meaning that no additional condition is required for a unique solution. The unknown constant  $a$  is then determined from the equilibrium condition (19). To solve the problem, first the equations are again normalized

by defining the new variables  $x_1, s_1, x_2, s_2$  as given by (50) and letting

$$\begin{aligned} \phi_1(s_1) = f_1(t) \quad , \quad \phi_2(s_2) = f_3(t) \quad , \quad \psi_1(x_1) = g_1(r) \quad , \\ \psi_2(x_2) = g_3(r). \end{aligned} \quad (58)$$

Then, the system of  $2n$  algebraic equations consisting of (54) and (55b) and

$$G_1(s_{1n}) = G_1(-1) = 0 \quad (59)$$

is solved for  $G_1(s_{1k})$  and  $G_2(s_{2k})$  for a specified value of the constant  $a$ . The corresponding value of the resultant force  $P$  is then obtained (in an inverse manner) by using the equilibrium condition (19) or

$$P = -\frac{b-a}{2} \int_{-1}^1 \phi_1(s_1) ds_1 \quad (60)$$

---

In the case of the edge crack, i.e., for  $c=0$ , basically the integral equations (12-14) or (28,29) and the kernels (16) remain the same. However, in this problem even though the equilibrium conditions such as (19,20) and (26) must still be satisfied, the single-valuedness condition (18) is no longer valid. The reason for this, of course, is that at  $r=0$   $u_\theta(r,0)$  is no longer zero and  $f_3(r)=\partial u_\theta/\partial r$  is nonzero, finite, and unknown. Also note that at  $r=0$  the asymptotic problem is that of an elastic wedge of angle  $\theta_0$ , ( $0 < \theta_0 \leq \pi$ ) for which  $\sigma_{ij}(r,\theta) \sim p_{ij} + O(r^\alpha)$  as  $r \rightarrow +0$ , ( $i,j=r,\theta; 0 \leq \theta \leq \theta_0$ ) where  $p_{ij}$  is a finite constant which is zero for wedges with stress-

free boundaries and the real constant  $\alpha$  is positive.\* In this case the numerical solution of the problem can be obtained by following the procedure outlined in this section with a minor change, namely by excluding the single-valuedness condition (55b) and by replacing it by the condition  $G_2(s_{2n})=0$ . Thus, considering (53b), at  $s_2=-1$  (or at  $r=0$ )  $\phi_2(s_2)$  becomes indeterminate and may be evaluated by extrapolation (if needed).

## 6. RESULTS AND DISCUSSION

The results for the wedge problem without the crack were given in [4] and [5]. However, in order to give some idea about the effect of the wedge angle and of the coefficient of friction on the stresses which may cause the formation of a crack, the stress distribution along  $\theta = 0$  plane is calculated. The results are shown in Figure 2. Based on these results, one could make two important observations, namely the existence of friction would inhibit crack initiation and, for relatively small wedge angles  $2\theta_0$ , as  $r$  increases the cleavage stress  $\sigma_{\theta\theta}(r,0)$  would

---

\*The statement in Ref. [7] (p. 619) regarding this point, namely "A simple residue calculation shows that the stresses are  $O(r^{-s^*-1})$  as  $r \rightarrow +0$ , where  $s^*$  is the first zero of  $\Delta(s, \theta_0) = s \sin 2\theta_0 + \sin 2s\theta_0$  to the left of zero. It is easily shown that as  $\theta_0$  increases from 0 to  $\pi$ ,  $s^*$  increases from  $-3/2$  to  $-1/2$ ," is clearly incorrect. It is valid only for a wedge of angle  $2\theta_0$  under symmetric loading, that is, in the present case, only for the uncracked wedge (see, equations 36a, 37, and 38, where  $s+1$  replaces  $s$  in [7]). Upon introducing the crack, the total wedge angle becomes  $\theta_0$ , ( $0 < \theta_0 \leq \pi$ ) and the stress singularity disappears.

change sign and would become negative. This means that for such wedge angles, even if the crack is formed, it would not propagate very far. The calculated stress intensity factors given in this paper also support this conclusion.

In the elastic wedge the practical problem is, of course, the edge crack problem. This is strongly demonstrated by the results for an internal crack given in Tables 2 and 3, and Figure 3. The stress intensity factors  $k(o)$ ,  $k(c)$ , and  $k(d)$  given in the tables and in the figure are defined by equations (39), (31a) and (31b), respectively. As the crack distance  $c/l$  increases, as indicated by Figure 3,  $k(o)$  quickly converges to the values given in [5] for the uncracked wedge. In the figure and in the tables  $k(o)$  is normalized with respect to  $P/(\pi e^{1-\omega})$ ,  $e = (b+a)/2$  and  $\omega = 2 + s_{-1}$  (see equations 38 and 39). The results given in tables 2 and 3 and Figure 3 show that as  $c \rightarrow 0$ ,  $k(o) \rightarrow \infty$  and  $k(c) \rightarrow \infty$ . Hence in brittle solids the most likely location of crack initiation would be the wedge apex. The tables also show the strength of singularity at  $r = a$  and  $r = b$  for the contact stress  $\sigma_{\theta\theta}(r, \theta_0)$ . Recalling the form of the contact stress given by (48), these stress concentration (or intensity) factors are defined by

$$k(a) = -\lim_{r \rightarrow a} \sqrt{r} (r-a)^{-\beta} \sigma_{\theta\theta}(r, \theta_0) ,$$

$$k(b) = -\lim_{r \rightarrow b} \sqrt{r} (b-r)^{-\alpha} \sigma_{\theta\theta}(r, \theta_0) . \quad (61 \text{ a,b})$$



Table 2. The results for the flat punch with sharp corners and the internal crack (see the insert in Figure 3),  $\xi = (b-a)/2$ ,  $e = (b+a)/2$ ,  $m = (d-c)/2$ ,  $\nu = 0.3$ ,  $\eta = 0.2$ .

$\theta_0$	$\frac{a}{\xi}$	$\frac{b}{\xi}$	$\frac{c}{\xi}$	$\frac{d}{\xi}$	$\frac{k(o)}{P/(\pi e l^{-\omega})}$	$\frac{k(a)}{P/(\pi \xi l^{1+\beta})}$	$\frac{k(b)}{P/(\pi \xi l^{1+\alpha})}$	$\frac{k(c)}{P/(\pi m^2)}$	$\frac{k(d)}{P/(\pi m^2)}$
150°	1.	3.	1.	2.	0.7791	1.1552	0.9069	0.1249	0.0913
150°	1.	3.	0.01	1.01	1.932	1.1300	0.9207	1.2239	0.2595
150°	1.	3.	0.001	1.001	5.436	1.1170	0.9267	2.9296	0.2927
150°	1	3	0	1		1.0796	0.9442		0.3846
165°	1.	3.	1.	2.	0.9795	1.2805	0.8259	0.1774	0.1285
165°	1.	3.	0.01	1.01	2.4399	1.2365	0.8487	1.6319	0.3598
165°	1.	3.	0.001	1.001	6.7059	1.2164	0.8580	3.8886	0.4035
165°	1	3	0	1		1.1573	0.8855		0.5251
150°	3.	5.	1.	2.	0.7437	1.0553	0.9571	0.1106	0.0837
150°	3.	5.	0.01	1.01	1.9466	1.0484	0.9618	0.8750	0.2087
150°	3.	5.	0.001	1.001	5.5051	1.0457	0.9636	2.0836	0.2323
165°	3.	5.	1.	2.	0.9269	1.1069	0.9158	0.1548	0.1186
165°	3.	5.	0.01	1.01	2.4097	1.0962	0.9231	1.1486	0.2816
165°	3.	5.	0.001	1.001	6.6521	1.0922	0.9258	2.7282	0.3123

Table 3. The results for the flat punch with sharp corners and the internal crack (see the insert in Figure 3),  $\lambda = (b-a)/2$ ,  $e = (b+a)/2$ ,  $m = (d-c)/2$ ,  $\nu = 0.3$ ,  $\eta = 0.5$ .

$\theta_0$	$\frac{a}{\lambda}$	$\frac{b}{\lambda}$	$\frac{c}{\lambda}$	$\frac{d}{\lambda}$	$\frac{k(o)}{P/(\pi e^{1-\omega})}$	$\frac{k(a)}{P/(\pi \lambda^{1+\beta})}$	$\frac{k(b)}{P/(\pi \lambda^{1+\alpha})}$	$\frac{k(c)}{P/(\pi m^2)}$	$\frac{k(d)}{P/(\pi m^2)}$
150°	1.	3.	1.	2.	0.4972	1.0486	0.9714	0.0796	0.0613
150°	1.	3.	0.01	1.01	1.1986	1.0326	0.9795	0.7520	0.1576
150°	1.	3.	0.001	1.001	3.3612	1.0244	0.9831	1.8088	0.1780
150°	1	3	0	1		1.0003	0.9935		0.2350
165°	1.	3.	1.	2.	0.8330	1.2211	0.8682	0.1570	0.1152
165°	1.	3.	0.01	1.01	2.0788	1.1820	0.8870	1.3898	0.3113
165°	1.	3.	0.001	1.001	5.7132	1.1641	0.8948	3.3126	0.3485
165°	1	3	0	1		1.1115	0.9174		0.4523
150°	3.	5.	1.	2.	0.4811	0.9954	0.9956	0.0660	0.0508
150°	3.	5.	0.01	1.01	1.2295	0.9910	0.9984	0.5493	0.1261
150°	3.	5.	0.001	1.001	3.4692	0.9893	0.9995	1.3119	0.1409
165°	3.	5.	1.	2.	0.7968	1.0669	0.9427	0.1344	0.1038
165°	3.	5.	0.01	1.01	2.0683	1.0574	0.9487	0.9852	0.2424
165°	3.	5.	0.001	1.001	5.7080	1.0538	0.9509	2.3407	0.2687

Without covering a wide range, the tables show the trends of various stress concentrations for varying crack distance  $(d+c)/2$ , punch distance  $(b+a)/2$ , wedge angle  $2\theta_0$ , and coefficient of friction  $\eta$ .

The results obtained for the edge crack ( $c=0$ ) are given by Figures 4-7 and Tables 4-9. For fixed relative dimensions  $d = a = \lambda$ ,  $(b-a=2\lambda)$  and for various values of the coefficient of friction  $\eta$ , Figure 4 shows the effect of the wedge angle  $2\theta_0$  on the stress intensity factor  $k(d)$ . It is seen that  $k(d)$  decreases as  $\eta$  increases or as  $\theta_0$  decreases, becoming eventually zero on a critical line in  $\eta$  vs.  $\theta_0$  plane. For fixed values of wedge angle ( $\theta_0=150^\circ$ ), crack length ( $d/a=1$ ), and coefficient of friction ( $\eta=0$ ,  $\eta=0.5$ ), the effect of the contact area as measured by  $b/a$  is shown in Figure 5. As  $b$  increases there is a slight reduction in the stress intensity factor  $k(d)$ . Figure 6 shows the effect of the coefficient of friction  $\eta$  on the stress intensity factor  $k(d)$  for fixed relative dimensions and for  $\theta_0 = 150^\circ, 165^\circ, 180^\circ$ . For  $\theta_0 = 180^\circ$  the change in  $k(d)$  (which is quite insignificant) comes primarily from the effect of  $\eta$  on the contact stress  $\sigma_{\theta\theta}(r, \theta_0)$ .

For the flat punch with sharp corners more detailed results are given in Tables 4-7. The negative  $k(d)$  values found for  $\theta_0 = 120^\circ$  in Table 4 indicate (from the fracture viewpoint) the beneficial effect of friction and should be

Table 4. The results for the wedge containing an edge crack loaded by a flat punch with sharp corners,  $\nu = 0.3$ ,  $a/\ell = 1$ ,  $b/\ell = 3$ ,  $\ell = (b-a)/2$ .

$\eta$	$\theta_0$	$\frac{k(a)}{P/(\pi\ell^{1+\beta})}$	$\frac{k(b)}{P/(\pi\ell^{1+\alpha})}$	$\frac{k(d)}{P/(\pi d^2)}$
0	120°	0.8832	1.0999	0.1133
0	150°	1.1267	0.9058	0.6876
0	165°	1.1826	0.8600	0.8123
0	172.5°	1.1946	0.8501	0.8391
0	180°	1.1981	0.8472	0.8472
0.2	120°	0.7935	1.1526	-0.1703
0.2	150°	1.0796	0.9442	0.5439
0.2	165°	1.1573	0.8855	0.7426
0.2	172.5°	1.1780	0.8699	0.8030
0.2	180°	1.1887	0.8620	0.8419
0.5	120°	0.6510	1.2197	-0.5834
0.5	150°	1.0003	0.9935	0.3323
0.5	165°	1.1115	0.9174	0.6396
0.5	172.5°	1.1459	0.8938	0.7495
0.5	180°	1.1676	0.8790	0.8340

Table 5. The results for the wedge containing an edge crack loaded by a flat punch with sharp corners,  $\nu = 0.3$ ,  $a/\ell = 1$ ,  $b/\ell = 3$ ,  $\theta_0 = 150^\circ$ , and  $\eta = 0$ .

$\frac{d}{\ell}$	$\frac{k(d)}{P/\pi\sqrt{\ell}}$	$\frac{k(a)}{P/(\pi\ell^{1+\beta})}$	$\frac{k(b)}{P/(\pi\ell^{1+\alpha})}$
0.001	0.8698	1.2192	0.8575
0.1	0.8803	1.2030	0.8648
0.2	0.8522	1.1892	0.8714
0.5	0.7767	1.1585	0.8874
1.	0.6876	1.1267	0.9058
2.	0.5803	1.0912	0.9279
3.	0.5145	1.0708	0.9416
4.	0.4683	1.0572	0.9511
5.	0.4332	1.0475	0.9583
6.	0.4053	1.0403	0.9638
7.	0.3824	1.0346	0.9683
8.	0.3630	1.0300	0.9719
9.	0.3464	1.0263	0.9750
10.	0.3319	1.0232	0.9776

Table 6. The results for the wedge containing an edge crack loaded by a flat punch with sharp corners,  $\nu = 0.3$ ,  $a/\ell = 1$ ,  $b/\ell = 3$ ,  $\theta_0 = 150^\circ$ , and  $\eta = 0.2$ .

$\frac{d}{\ell}$	$\frac{k(d)}{P/\pi\sqrt{\ell}}$	$\frac{k(a)}{P/(\pi\ell^{1+\beta})}$	$\frac{k(b)}{P/(\pi\ell^{1+\alpha})}$
0.001	0.6950	1.1550	0.9067
0.1	0.6975	1.1417	0.9124
0.2	0.6729	1.1304	0.9176
0.5	0.6118	1.1054	0.9300
1.	0.5439	1.0796	0.9442
2.	0.4647	1.0505	0.9615
3.	0.4163	1.0336	0.9723
4.	0.3818	1.0223	0.9799
5.	0.3553	1.0141	0.9856
6.	0.3340	1.0080	0.9900
7.	0.3162	1.0032	0.9936
8.	0.3011	0.9993	0.9966
9.	0.2880	0.9962	0.9991
10.	0.2765	0.9935	1.0012

Table 7. The results for the wedge containing an edge crack loaded by a flat punch with sharp corners,  $\nu = 0.3$ ,  $a/\ell = 1$ ,  $b/\ell = 3$ ,  $\theta_0 = 150^\circ$ , and  $\eta = 0.5$ .

$\frac{d}{\ell}$	$\frac{k(d)}{P/\pi\sqrt{\ell}}$	$\frac{k(a)}{P/(\pi\ell^{1+\beta})}$	$\frac{k(b)}{P/(\pi\ell^{1+\alpha})}$
0.001	0.4430	1.0484	0.9713
0.1	0.4336	1.0397	0.9748
0.2	0.4134	1.0324	0.9779
0.5	0.3712	1.0166	0.9852
1.	0.3323	1.0003	0.9936
2.	0.2930	0.9817	1.0039
3.	0.2697	0.9705	1.0105
4.	0.2525	0.9628	1.0153
5.	0.2387	0.9572	1.0189
6.	0.2270	0.9530	1.0218
7.	0.2170	0.9496	1.0242
8.	0.2082	0.9469	1.0261
9.	0.2004	0.9446	1.0278
10.	0.1934	0.9427	1.0292

disregarded. Tables 5-7 show the stress intensity factors as a function of the crack length  $d$ . The important conclusion which may be drawn from these results is that for a fixed driving force  $P_0$ ,  $k(d)$  is a decreasing function of  $d$ . Therefore, the related brittle fracture process is expected to be stable.

Finally, Table 8 and 9 and Figure 7 show some results for an elastic wedge containing an edge crack and loaded by a blunted punch. The punch profile is rounded in the neighborhood of  $r = a$  and has a radius of curvature  $R$  (see equation (57)). The trailing edge of the punch,  $r = b$  is sharp. Figure 7 shows a sample result giving the resultant contact force  $P$  and the stress intensity factor  $k(d)$  as a function of the relative change in the contact area  $(a_0 - a)/R$ . The numerical results for two punch sizes are given in Tables 8 and 9.

In calculating the results the basic computer program was run by using the input parameters for known special cases for the purpose of verification. The comparison, whenever possible, was quite satisfactory. For example, in the case of an edge crack with  $\theta_0 = 180^\circ$  the problem is that of a wedge-loaded semi-infinite crack. In the punch-loaded wedge problem letting  $a/\ell = 99$ ,  $b/\ell = 101$ ,  $d/\ell = 100$ ,  $\ell = (b-a)/2$ , it was found that  $k(d)/[P/(\pi\sqrt{d})] = 0.999995$  whereas the exact value is 1 (more specifically,



Table 8. The results for an elastic wedge containing an edge crack and loaded by a blunted punch,  $\nu = 0.3$ ,  $\eta = 0.5$ ,  $\theta_0 = 165^\circ$ ,  $a_0 = R$ ,  $d = R$ , and  $b = 2R$ .

$\frac{a_0 - a}{R}$	$\frac{1 + \kappa}{4\mu} \frac{P}{R}$	$\frac{k(b)}{P/R^{\alpha+1}}$	$\frac{k(d)}{P/d^2}$
0.5	0.5990	0.3742	0.1891
0.4	0.4225	0.3833	0.1881
0.3	0.2710	0.3932	0.1871
0.2	0.1460	0.4037	0.1861
0.1	0.0515	0.4149	0.1852
0.05	0.0186	0.4210	0.1847
0.02	0.0048	0.4246	0.1845

Table 9. The results for an elastic wedge containing an edge crack and loaded by a blunted punch,  $\nu = 0.3$ ,  $\eta = 0.5$ ,  $\theta_0 = 165^\circ$ ,  $a_0 = R$ ,  $d = R$ , and  $b = 3R$ .

$\frac{a_0 - a}{R}$	$\frac{1+\kappa}{4\mu} \frac{P}{R}$	$\frac{k(b)}{P/R^{\alpha+1}}$	$\frac{k(d)}{P/d^2}$
0.5	0.7108	0.2711	0.2123
0.4	0.5134	0.2757	0.2102
0.3	0.3366	0.2802	0.2084
0.2	0.1851	0.2848	0.2067
0.1	0.0764	0.2897	0.2050
0.05	0.0246	0.2922	0.2042
0.02	0.0066	0.2938	0.2037

$k = \sqrt{2P}/(\pi\sqrt{c_1})$ ,  $c_1$  being the distance of the concentrated wedge force  $P$  from the crack tip).

## REFERENCES

1. H. Neuber, Theory of Notch Stresses, J. W. Edwards, Ann Arbor, Michigan, 1946.
2. M.L. Williams, "Stress singularities resulting from various boundary conditions in angular corners of plates in extension", Trans. ASME, Vol. 74, p. 625, 1952.
3. E. Sternberg and W.T. Koiter, "The wedge under concentrated couple: a paradox in the two-dimensional theory of elasticity", J. Appl. Mech., Vol. 25, Trans. ASME, p. 575, 1958.
4. F. Erdogan and K. Arin, "Fracture and contact problems for an elastic wedge", Journal of Elasticity, Vol. 6, p. 57, 1976.
5. F. Erdogan and K. Arin, "Effect of friction in wedging of elastic solids", Journal of Elasticity, Vol. 6, p. 261, 1976.
6. F. Erdogan and H. Terada, "Wedge-loading of a semi-infinite strip with an edge crack", to appear in Int. J. of Fracture, 1978.
7. L.M. Keer, D.A. Mendelsohn, and J.D. Achenbach, "Crack at the apex of a loaded notch", Int. J. Solids, Structures, Vol. 13, p. 615, 1977.
8. V.L. Hein and F. Erdogan, "Stress singularities in a two-material wedge", Int. J. Fracture Mechanics, Vol. 7, p. 317, 1971.
9. F. Erdogan, "Mixed Boundary Value Problems in Mechanics", Mechanics Today, S. Nemat-Nasser, ed. Vol. 4, p. 1, 1978.
10. T.S. Cook and F. Erdogan, "Stresses in bonded materials with a crack perpendicular to the interface", Int. J. Engng. Sci., Vol. 10, p. 677, 1972.

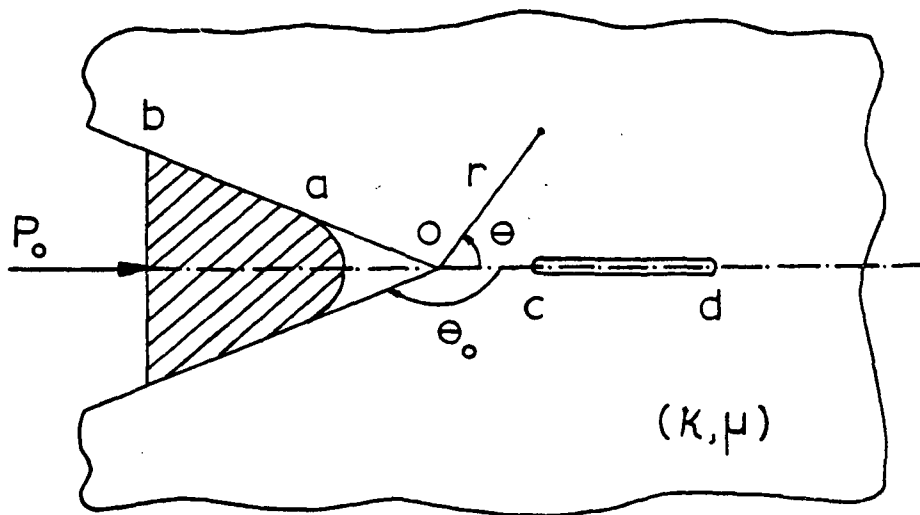


Figure 1. Basic geometry of the crack-contact problem.

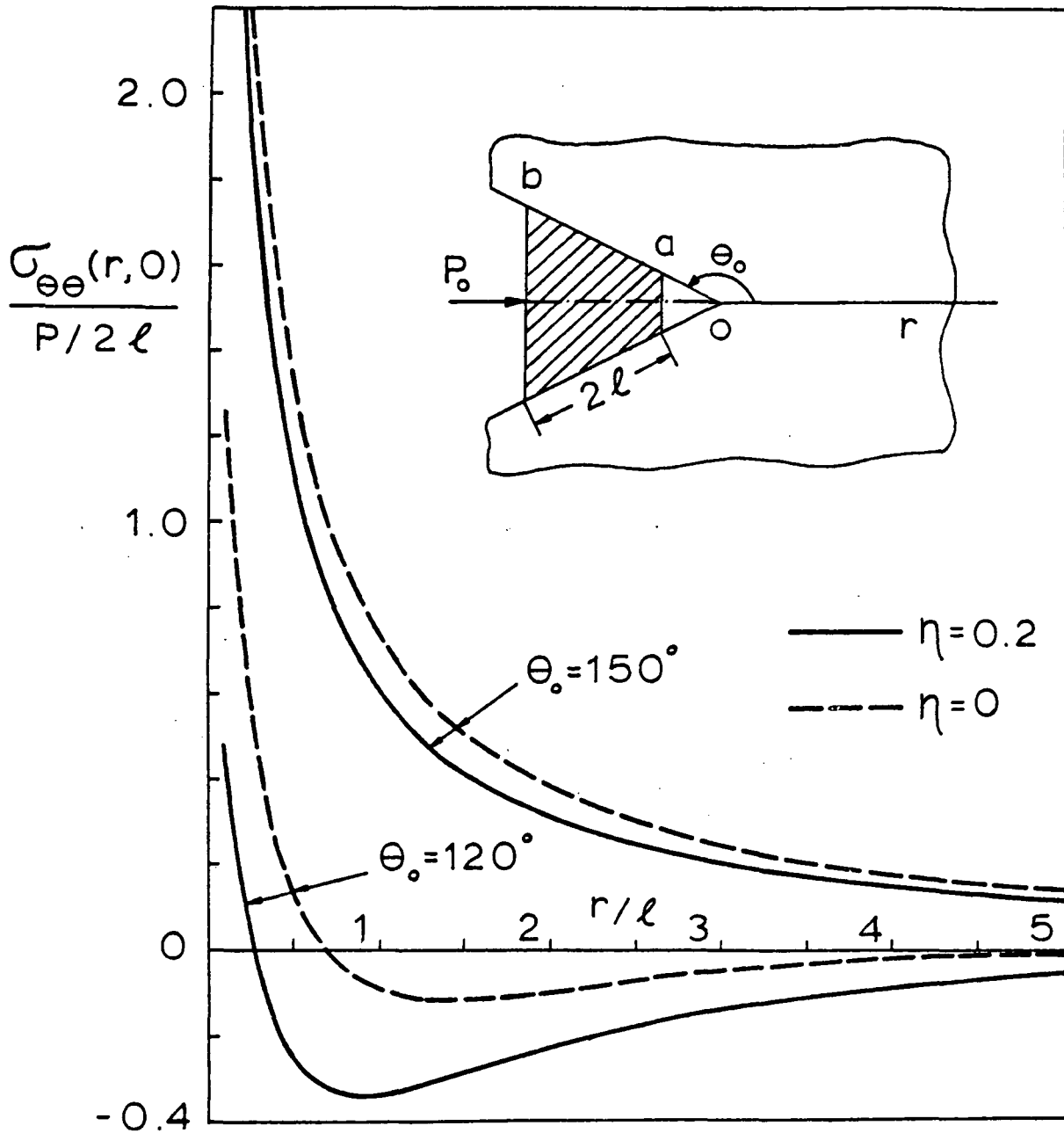


Figure 2. Distribution of the cleavage stress in a punch-loaded elastic wedge,  $a/\ell = 1$ ,  $b/\ell = 3$ ,  $\ell = (b-a)/2$ ,  $\eta$ : the coefficient of friction.

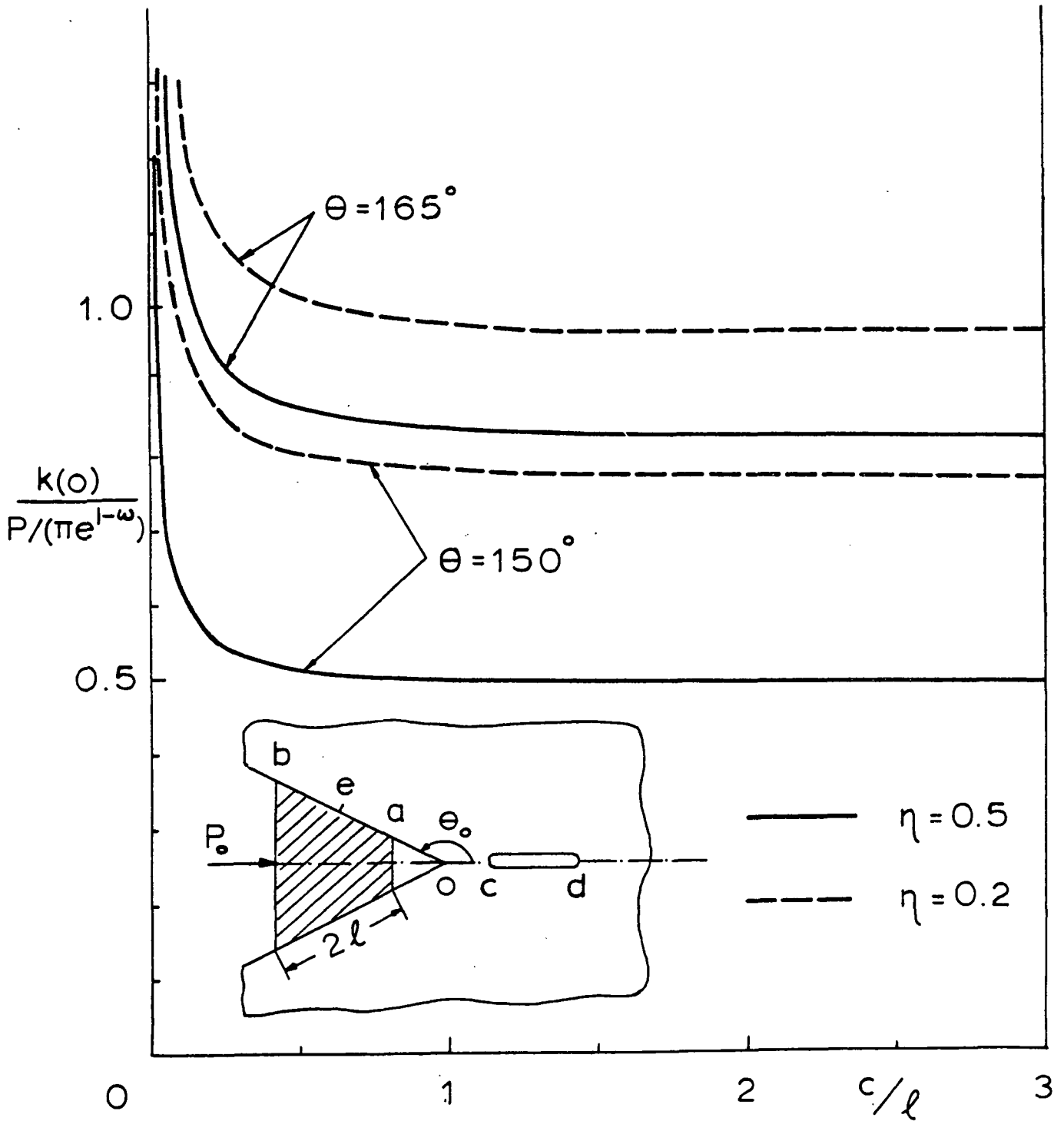


Figure 3. Variation of the strength of stress singularity at the wedge apex with the crack distance,  $a/\ell = 1$ ,  $b/\ell = 3$ ,  $(d-c)/\ell = 1$ , the normalization factor:  $k_0 = P/(\pi e^{1-\omega})$ ,  $\ell = (b-a)/2$ ,  $e = (b+a)/2$ .

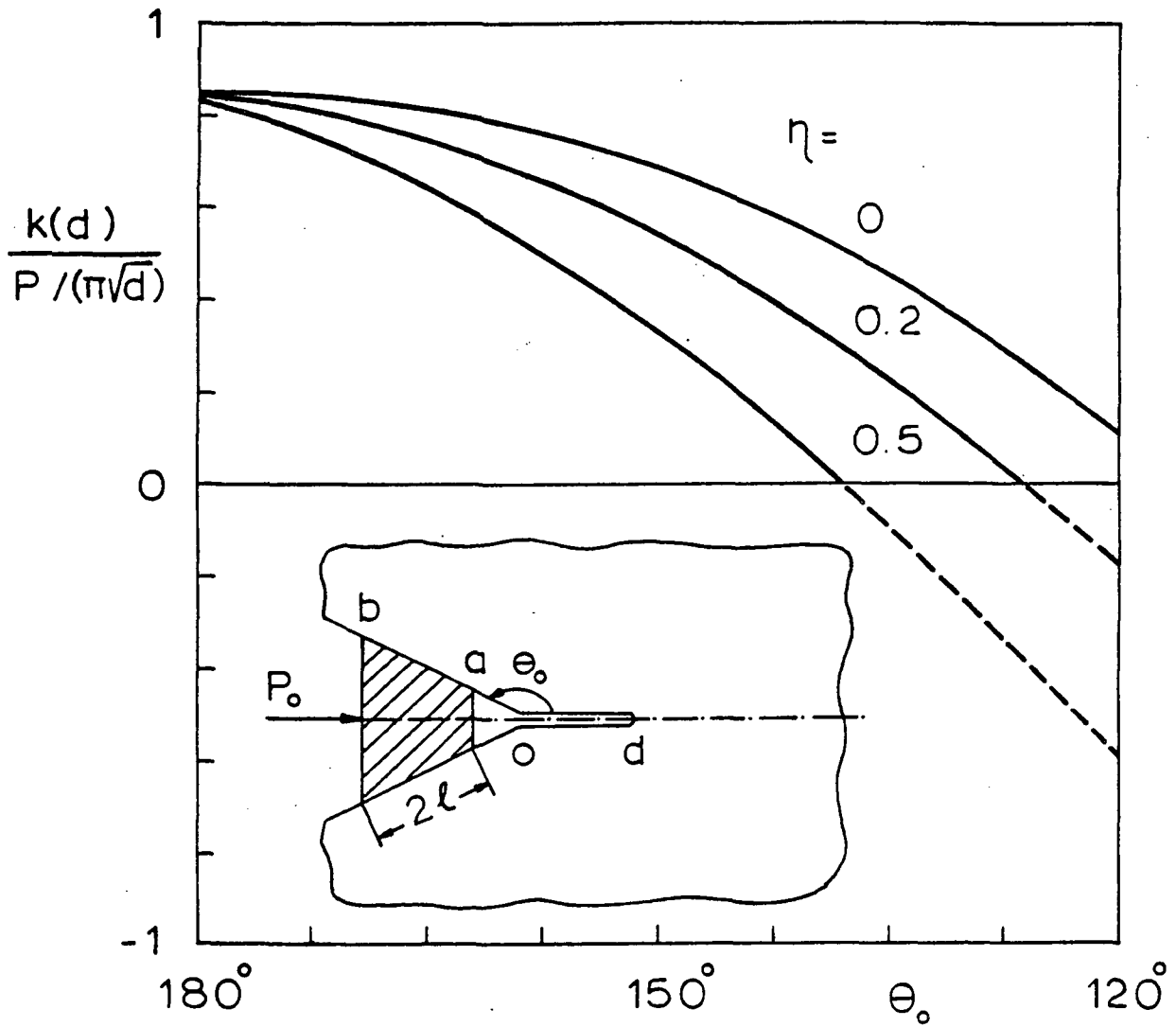


Figure 4. Variation of the stress intensity factor at the crack tip with the half-wedge angle  $\theta_0$  for various coefficients of friction  $\eta$ ,  $\nu = 0.3$ ,  $d = a = l$ ,  $l = (b-a)/2$ .



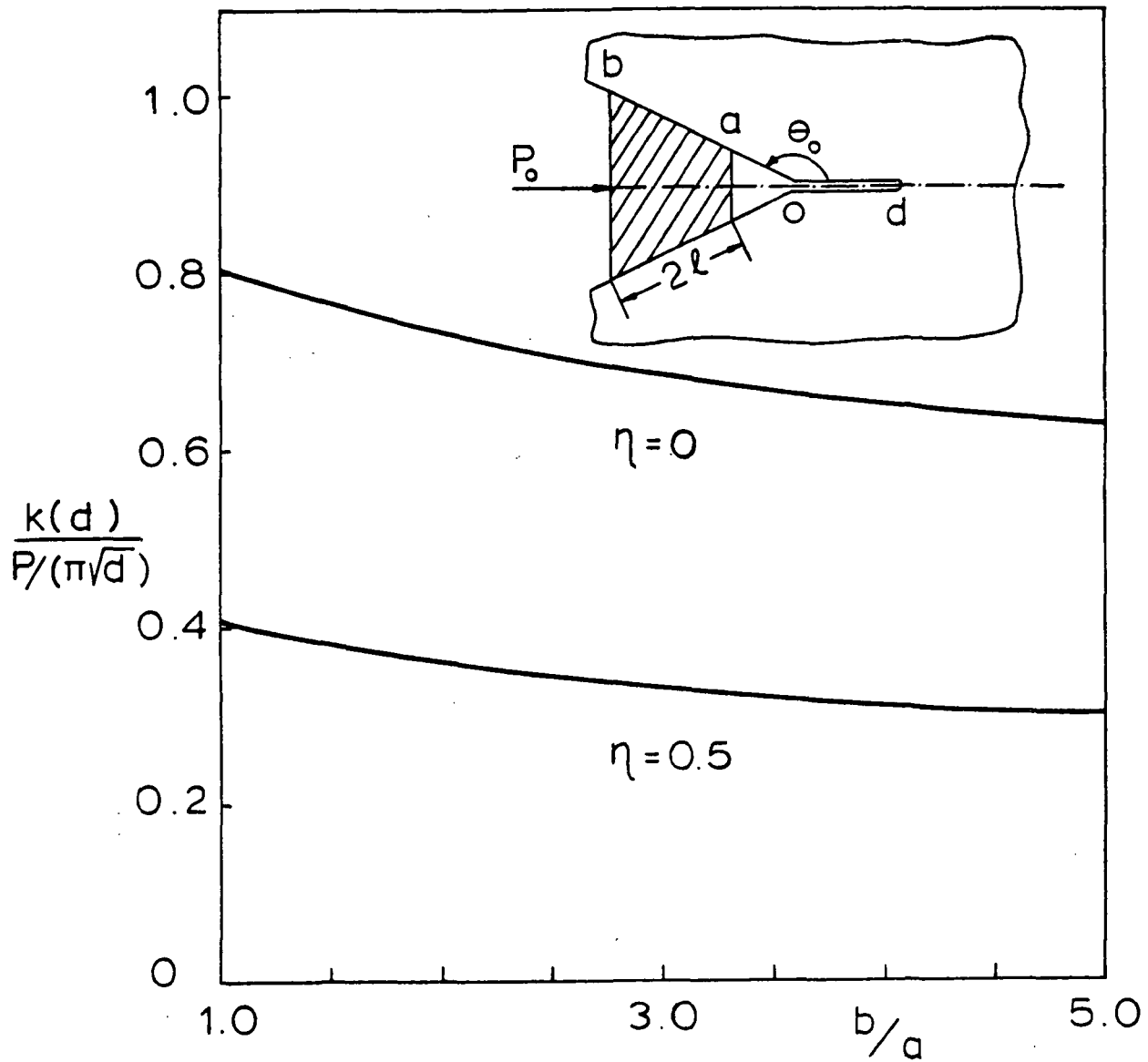


Figure 5. Variation of the stress intensity factor  $k(d)$  with the punch size,  $\theta_0 = 150^\circ$ ,  $d/a = 1$ ,  $\eta$ : the coefficient of friction.

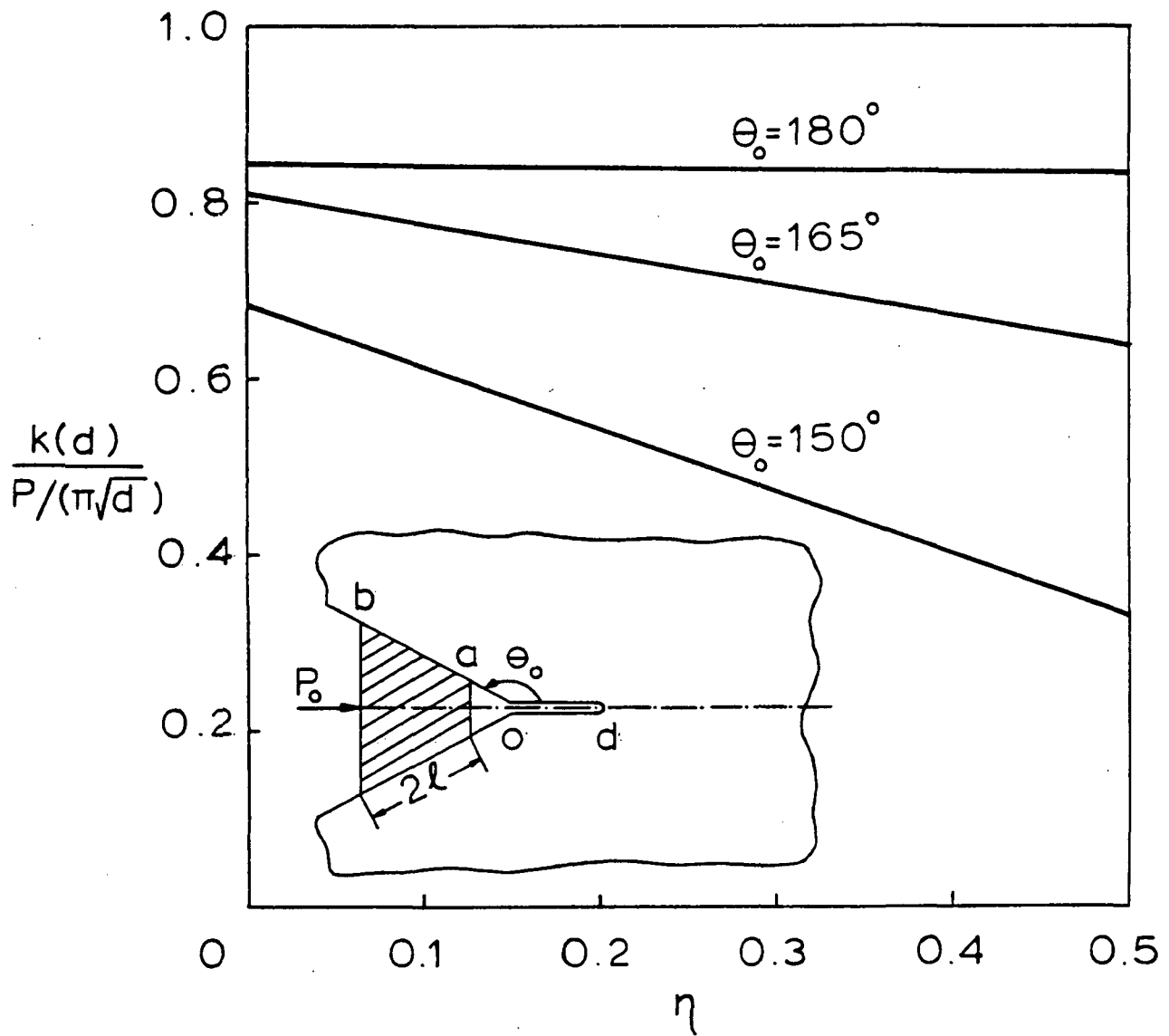


Figure 6. Variation of the stress intensity factor  $k(d)$  with the coefficient of friction  $\eta$ ,  $\nu = 0.3$ ,  $d = a$ ,  $b = 3a$ .

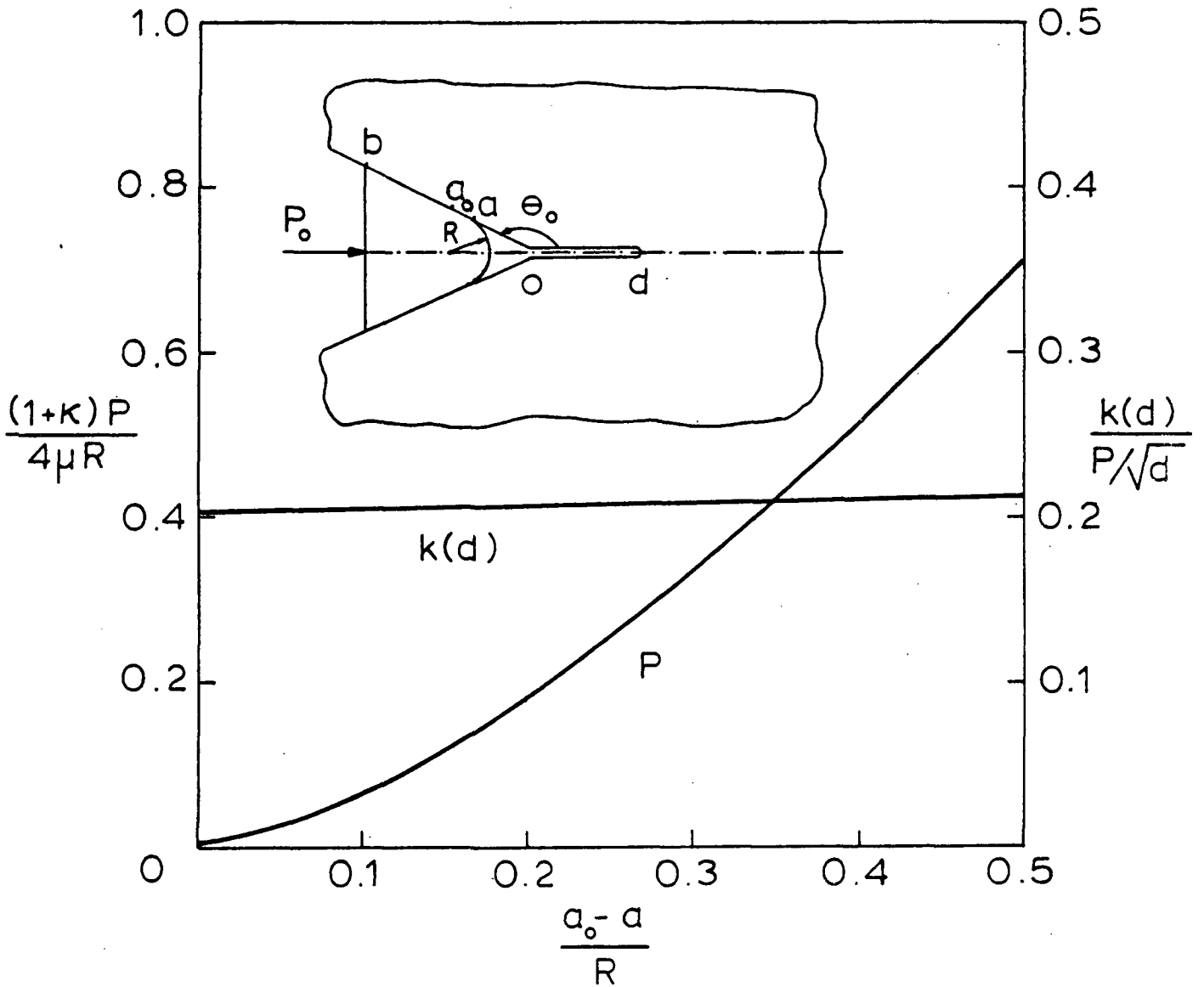


Figure 7. Stress intensity factor  $k(d)$  and the resultant contact force  $P$  as functions of the relative change in the contact area.  $P = 0$  for  $a = a_o$ ,  $a_o$  is the point of tangency on the punch profile.  $\nu = 0.3$ ,  $\eta = 0.5$ ,  $\theta_o = 165^\circ$ ,  $a_o = R$ ,  $d = R$ ,  $b = 3R$ .